Fall 21-3-2008

In vivo measurement of internal and global macromolecular motions in E. coli

M. Jasnin
Institut Laue Langevin, France

M. Moulin
Institut Laue Langevin, France

M. Haertlein
Institut Laue Langevin, France

G. Zaccai
Institut Laue Langevin, France

M. Tehei
University of Wollongong, moeava@uow.edu.au

In vivo measurement of internal and global macromolecular motions in E. coli

Abstract

We present direct quasielastic neutron scattering measurements, in vivo, of macromolecular dynamics in E. coli. The experiments were performed on a wide range of time-scales, to cover the large panel of internal and self-diffusion motions. Three major internal processes were extracted at physiological temperature: a fast picosecond (ps) process that corresponded to restricted jump diffusion motions, and two slower processes that resulted from reorientational motions occurring in about 40 ps and 90 ps, respectively. The analysis of the fast process revealed that the cellular environment leads to an appreciable increase in internal molecular flexibility and diffusive motion rates compared to those evaluated in fully hydrated powders. The result showed that the amount of cell water plays a decisive role in internal molecular dynamics. Macromolecular interactions and confinement, however, attenuate slightly the lubricating effect of water, as revealed by the decrease of the in vivo parameters compared to those measured in solution. The study demonstrated that standard sample preparations do not mimic accurately the physiological environment, and suggested that intracellular complexity participates in functional dynamics necessary to biological activity. Furthermore, the method allowed the extraction of the self-diffusion of E. coli macromolecules, which presented similar parameters as those extracted for hemoglobin in red blood cells.

Keywords

Neutron scattering, Quasielastic, In vivo dynamics, Internal molecular motions, Self-diffusion, Macromolecular crowding

Publication Details

This article was originally published as Jasnin, M, Moulin, M, Haertlein, M, Zaccai, G, and Tehei, M, In vivo measurement of internal and global macromolecular motions in E.coli. Biophysical Journal, 95, 2008, 857-864. Copyright The Biophysical Society 2008. Original journal available here

Biophys J BioFAST, published on March 21, 2008 as doi:10.1529/biophysj.107.124420

Corresponding Author: Zaccai Giuseppe, Institut Laue Langevin, 6 rue Jules Horowitz, BP 156, 38042 Grenoble Cedex 9, France
Tel: +33476207679, Fax: +33476207120
Email: zaccai@ill.fr

In vivo measurement of internal and global macromolecular motions in *E. coli*

Jasnin M.[*,§], Moulin M.[#], Haertlein M.[#], Zaccai G.[*,§] and Tehei M.[§]

[*] Institut de Biologie Structurale, Laboratoire de Biophysique Moléculaire, Grenoble, France
[#] Institut Laue Langevin, Deuteration Laboratory, Grenoble, France
[§] Institut Laue Langevin, Grenoble, France

ABSTRACT

We present direct quasielastic neutron scattering measurements, *in vivo,* of macromolecular dynamics in *E. coli*. The experiments were performed on a wide range of time-scales, to cover the large panel of internal and self-diffusion motions. Three major internal processes were extracted at physiological temperature: a fast picosecond (ps) process that corresponded to restricted jump diffusion motions, and two slower processes that resulted from reorientational motions occurring in about 40 ps and 90 ps, respectively. The analysis of the fast process revealed that the cellular environment leads to an appreciable increase in internal molecular flexibility and diffusive motion rates compared to those evaluated in fully hydrated powders. The result showed that the amount of cell water plays a decisive role in internal molecular dynamics. Macromolecular interactions and confinement, however, attenuate slightly the lubricating effect of water, as revealed by the decrease of the *in vivo* parameters compared to those measured in solution. The study demonstrated that standard sample preparations do not mimic accurately the physiological environment, and suggested that intracellular complexity participates in functional dynamics necessary to biological activity. Furthermore, the method allowed the extraction of the self-diffusion of *E. coli* macromolecules, which presented similar parameters as those extracted for hemoglobin in red blood cells.

Keywords: Neutron scattering, Quasielastic, *In vivo* dynamics, Internal molecular motions, Self-diffusion, Macromolecular crowding

INTRODUCTION

The study of internal molecular motions on the pico- to nanosecond (ps-ns) time-scale reveals fundamental dynamical processes required for biological activity and stability. Ps-ns local motions in macromolecules act as the lubricant of larger conformational changes on a slower, millisecond, time-scale (1) that are necessary for important biological processes, including ligand binding, intermolecular recognition, enzyme catalysis and signal transduction (2-5). Incoherent neutron scattering spectroscopy is a powerful technique for the measurement of atomic motions on the ps-ns time domain. The scattering signal is dominated by hydrogen nuclei, which have a neutron incoherent cross section about forty times larger than the cross section of any other nucleus or isotope. Hydrogen atoms represent up to about half of the atoms in biological macromolecules and are distributed nearly homogeneously within the structures. Their incoherent scattering signal, therefore, reflects internal molecular motions. Neutron studies have revealed that local molecular motions are influenced by environmental conditions, including hydration level and temperature. The temperature dependence of the global atomic mean square displacement (MSD), which corresponds to internal flexibility, has been studied extensively over the last decades (reviewed by (6)). At sufficient hydration, it has been found that, below a dynamical transition temperature at about 180-240 K, atomic motions are harmonic predominantly. The atoms are anchored within the structure, stacked in a given energy state, and they vibrate about their equilibrium position. Above the dynamical transition temperature, the MSD increases significantly due to the contribution of diffusive motions, which may contribute to the sampling of different conformational substates (7). At physiological conditions, the energy barrier separating different free energy states is similar to thermal energy, and the molecular subgroups can overcome rotational barriers. Many but not all macromolecules become fully active and functional only when these diffusive motions can take place. The study of localized diffusive motions, therefore, is of fundamental relevance to understand the origin of functional internal flexibility in macromolecules.

Quasielastic incoherent neutron scattering (QENS) provides accurate information on local diffusive motions occurring in macromolecules (8). The technique has been used extensively to study internal molecular motions in hydrated protein powders (9-16) as well as in the integral membrane protein bacteriorhodopsin in purple membrane stacks (17-21). These studies have indicated that internal flexibility decreased when the hydration level was lowered. Pérez and coworkers have compared internal dynamics in dry powder, at several hydration levels, and in solution, for myoglobin and lysozyme (16). They have shown that the surface side chains of the two types of proteins acquired progressively the possibility to diffuse locally, when increasing the hydration level up to complete coverage. Furthermore, both motion amplitudes and internal diffusive motion rates increased significantly in solution compared to fully hydrated powder. The differences in internal dynamics observed between powder and solution samples lead to another challenging question: what about the internal dynamics in the cell interior? Cell macromolecules move and interact in a crowded intracellular matrix. It has been shown that macromolecular self-diffusion coefficients are reduced in the cell cytoplasm (22-25), while macromolecular associations can be favoured (26). Very little is known concerning *in vivo* internal macromolecular dynamics. In particular, to what extent internal dynamics could be enhanced or reduced under cellular conditions of hydration and crowding, compared to that measured in hydrated powder or in solution? In the present study, we addressed this question using QENS, and we present direct measurements of global and internal molecular motions in living *E. coli* at physiological temperature.

MATERIALS AND METHODS

Sample preparation

Native *E. coli* (BLE21 (DE3) strain) were cultivated at 37°C to an optical density value of 2, in Enfors minimum growth medium with glycerol as the carbon source. Cells were pelleted by centrifugation at 5000 x rpm in a Beckman centrifuge (JLA 10500 rotor) for 20 minutes at 4°C. The supernatant was discarded and the cells were washed twice with 100 ml of D_2O buffer solution (150 mM NaCl, 5 mM KCl, 10 mM Tris-DCl pH 6.6). The cells were pelleted via 20 minutes centrifugation and transferred to aluminium sample holders (4 x 3 x 0.03 cm^3). After the experiments, a small amount of the pellet was resuspended in the buffer and layered on Petri dishes after several dilutions steps. The number of colonies was compared to that obtained for cells from the fresh culture, and found to be similar, which indicated that most of the cells remained intact and viable after the total beamtime exposure.

Neutron scattering measurements

The experiments were carried out at room temperature using three spectrometers: the time-of-flight spectrometer IN6 (Institut Laue Langevin (ILL), Grenoble; see www.ill.fr for further information), with an energy resolution of 90 μeV (full-width at half-maximum, FWHM); the inverted time-of-flight spectrometer IRIS (Rutherford Appleton Laboratory, Chilton, see www.isis.rl.ac.uk), with an energy resolution of 17 μeV (FWHM); and the backscattering spectrometer IN16 (ILL, Grenoble, FWHM = 0.9 μeV). The scattering was measured over a wave-vector of 0.5 $Å^{-1} < Q < 1.7$ $Å^{-1}$ (Q is the wave vector transfer modulus). A vanadium sample (a purely elastic scatterer) was measured to define the instrument resolution and correct for detector efficiency. IRIS, IN6 and IN16 spectra were corrected for detector efficiency, sample container and buffer scattering, normalized, grouped, and converted to $S(\mathbf{Q},\omega)$ data using the MODES and LAMP data reduction routines (27, 28), respectively. The transmissions of the samples were > 90 % and multiple scattering was neglected.

Incoherent neutron scattering from living cells

An exhaustive description of quasielastic incoherent neutron scattering (QENS) can be found in Bée (29). Hydrogen nuclei have an incoherent cross section forty times larger than that of any other atom and isotope, and they dominate the scattering signal. As the signal relies on incoherent scattering, the dynamics of hydrogenated molecules can be explored in samples that need not be crystalline or even monodisperse, such as living cells (30). Macromolecules make up *ca*. 96 % of the total dry weight of *E. coli*, of which 55 % are proteins, 20 % are ribonucleic acids (RNA) and 9 % are lipids (see Table 1) (31). Internal motions of *E. coli* macromolecules were studied by measuring native (natural abundance of H) *E. coli* resuspended in D_2O buffer. A subtraction of the D_2O buffer spectra from the spectra measured for the cells gives a valuable approximation of the scattering signal from cell macromolecules. Considering that proteins are the dominant cellular macromolecules by mass and that the hydrogen percentage is higher in proteins compared to every other type of macromolecules (about 50 % for proteins compared to 30 % for RNA and lipids), it is reasonable to assume, therefore, that protein motions dominate the macromolecular scattering signal from living cells.

Separation of the diffusive motions using QENS

The diffusive motions of hydrogen atoms in macromolecules explored here belong to the ps-ns time domain, and can be detected using the combination of different neutron spectrometers. The energy resolution of the spectrometer defines the upper limit of the

accessible times of motions. The IN6 spectrometer, which has a FWHM = 90 μeV, is suitable for the measurement of motions with short characteristic times, τ < 15 ps. The higher resolution of the IRIS spectrometer, FWHM = 17 μeV, resolves slower motions, with τ < 75 ps. Very slow motions that occur up to about 1 ns can be detected with the very high energy resolution of IN16 (FWHM = 0.9 μeV). On each spectrometer, the average dynamical behaviour of all protons diffusing in the time-window is measured. The protons, which move very slowly with respect to the time-scale associated to the spectrometer, are seen as immobile and contribute to the elastic intensity. On the reverse, very fast protons with respect to the energy resolution contribute in a flat background.

Data analysis

In the quasielastic region of the measured spectra, the calculated scattering function, $S_{calc}(\mathbf{Q},\omega)$, has been described by Bée (29):

$$S_{calc}(\mathbf{Q},\omega) = DW \cdot S_{diff}(\mathbf{Q},\omega) \quad (1)$$

where DW is a Debye-Waller (DW) factor, which accounts for vibrational modes, and $S_{diff}(\mathbf{Q},\omega)$ is a diffusive contribution. The DW factor is simply a scaling factor in ω-space, which does not modify the shape of the quasielastic scattering function. In the case of global and internal macromolecular motions in the cell interior, $S_{calc}(\mathbf{Q},\omega)$ can be written as follows (29):

$$S_{calc}(\mathbf{Q},\omega) = DW\left[S_{self}(\mathbf{Q},\omega) \otimes \left(A_0(\mathbf{Q})\,\delta(\omega) + \sum_{i=1}^{n} A_i(\mathbf{Q})\,L(\Gamma_i,\omega)\right)\right] \quad (2)$$

The quasielastic component arises from the convolution of the self-diffusion scattering function, $S_{self}(\mathbf{Q},\omega)$, with the internal (localized) scattering function, $A_0(\mathbf{Q})\,\delta(\omega) + \sum_{i=1}^{n} A_i(\mathbf{Q})\,L(\Gamma_i,\omega)$, which are supposed to uncoupled from each other as has been done in previous work on myoglobin in crowded solutions (32). The global and internal scattering functions are both described by Lorentzian functions:

$$L(\Gamma_i,\omega) = \frac{1}{\pi}\frac{\Gamma_i(\mathbf{Q})}{\Gamma_i(\mathbf{Q})^2 + \omega^2} \quad (3)$$

with Γ_i the half-width at half-maximum (HWHM) of the Lorentzian peak.

The measured scattering function, $S_{meas}(\mathbf{Q},\omega)$, is obtained by convoluting $S_{calc}(\mathbf{Q},\omega)$ with the energy resolution of the spectrometer, $S_{res}(\mathbf{Q},\omega)$, determined by the vanadium sample:

$$S_{meas}(Q,\omega) = e^{-\hbar\omega/(2k_BT)}\left[S_{calc}(Q,\omega) \otimes S_{res}(Q,\omega)\right] + B_0 \quad (4)$$

in which $e^{-\hbar\omega/(2k_BT)}$ is a detailed balance factor and B_0 an inelastic background due to vibrational modes of lowest energy, which reminds the phonons in crystals (29).

For IRIS spectra, the fits were performed over the energy transfer range -0.2 to +0.5 meV, by using the IRIS Bayesian fitting program *QL function* present in the MODES package (27). The IN16 and IN6 spectra were fitted over the energy transfer ranges -12 μeV to +12 μeV and -1.5 meV to +1.5 meV, respectively, using the QENS_FIT routine present in the LAMP package (28).

RESULTS & DISCUSSION

Internal motions in living cells by QENS

In biological macromolecules, many different molecular substructure groups experience localized diffusive motions, which occur, in a large part, with correlation times from 0.1 to 200 ps (18). As described in *Materials and Methods*, the diffusive motions are related to the Lorentzian functions used to fit QENS data (see Data Analysis). The motions are characterized by the Lorentzian half-widths at half-maximum (HWHM), Γ_i, which are related at high Q^2 values to the inverse of correlation times, $\tau_{cor,i}$, and by quasielastic incoherent structure factors (QISF), A_i with i>0. A Q^2-independent linewidth can account for reorientational motions such as jump diffusion motions between a finite number of sites. In contrast, a non zero extrapolated value of Γ_i at $Q^2 = 0$, followed by an increase of the linewidth with Q^2, reflects diffusive motions within a confined volume. The EISF, which corresponds to the elastic intensity fraction over the total intensity, allows to access the motion geometry as well as the number of the mobile and immobile protons in the experimental energy resolution. The Q-dependences of Γ_i and the EISF, therefore, provide information on the nature of the motions.

With the aim of capturing the essence of the complex landscape of internal motions in cell macromolecules, we used a finite number of Lorentzians to parameterize the major types of motions depending on their time-scale. The interest was to describe the diffusive motions in a simplified and meaningful way, using only a few phenomenological variables. Each Lorentzian must be understood as an average contribution of the motions that occur in a certain time- and length-scales. In the following section, we described the motions belonging to the ps-to-ns time-scale, using the three instrumental energy resolutions presented previously. The characteristic length and time parameters of the motions were extracted from the Lorentzian HWHM and EISF as functions of Q, using both a phenomenological approach and accurate models. The aim of the approach was to determine whether or not internal macromolecular dynamics measured in entire cells was similar to that found in hydrated powder, in membrane or in solution, and to address to what extent the cellular environment influences the diffusive motions in macromolecules.

Fast internal motions

The internal motions captured on IN6 possess characteristic times of a few ps. On this time-scale, the global motions contribute to the scattering function as a very sharp Lorentzian that is much narrower than the instrumental energy resolution. Eq. 2 simplifies therefore as follows:

$$S_{calc}(\mathbf{Q},\omega) = DW\left[A_0(\mathbf{Q})\,\delta(\omega) + \sum_{i=1}^{n} A_i(\mathbf{Q})\,L(\Gamma_i,\omega) \right] \qquad (5)$$

The data were fitted with a single Lorentzian function using Eq. 4, 5. The QENS spectra and applied fits are plotted in Fig. 1. Considering the large number of molecular subunits that gives rise to a large variety of motions, the single Lorentzian analysis is a rough approximation; it gives, however, a good indication on the average motion type. The Q^2-dependence of the Lorentzian half-width at half-maximum (HWHM), Γ_{fast}, is plotted in Fig. 2. Γ_{fast} revealed the existence of diffusive motions within confined space, as indicated by the non-zero intercept, Γ_{f0}, in the low Q^2 region. Γ_{f0} is about 100 μeV at 280 K and 300 K. The low Q^2 profile was well accounted for by the model of Volino and Dianoux, which describes diffusion inside the volume of a sphere (33). The model gave access to the confinement sphere radius. Γ_{f0} follows (33):

$$\Gamma_{f0}(0 < Q < Q_0 = \pi/a) = \frac{4.33 D_{local}}{a^2} \quad (6)$$

where D_{local} is the diffusion coefficient inside a spherical volume of radius a. a was extracted from the EISF variation with Q. The model predicts that the experimental EISF follows:

$$\mathrm{EISF}(\mathbf{Q}) = \mathrm{p} + (1-\mathrm{p})\left\{\frac{3[\sin(Qa) - (Qa)\cos(Qa)]}{(Qa)^3}\right\}^2 \quad (7)$$

with p the fraction of immobile protons, with respect to the instrumental time-window. The Q-dependence of the EISF is plotted in Fig. 3. We found p = 0.61 and a = 3.11 Å at 280 K; p = 0.56 and a = 3.40 Å at 300 K. As revealed by the EISF profile at high Q values, the values of immobile protons, p, have large uncertainties. The fit is improved by using a distribution of radii of sphere. The approach with a single sphere radius was chosen to compare with previous work analysed in the same way.

At larger Q^2 values, the linewidth follows the well known jump diffusion behaviour (29). Γ_{fast} increases to approach asymptotically a constant value, $\Gamma_{f\infty}$. $\Gamma_{f\infty}$ is about 140 μeV at 280 K and 185 μeV at 300 K, which correspond to correlation times, $1/\Gamma_{f\infty}$, of about 4.7 ps and 3.6 ps, respectively.

Previous studies performed on hydrated powder at full hydration (hydration level h ~ 0.4 g water /g protein) and in solution have revealed similar Q^2-dependences for the single Lorentzian analysis (15-17, 19, 21, 34, 35). The characteristic parameters, however, appeared to be dependent of the sample type. The length-scale explored by the motions in cell macromolecules, given by the sphere radius of about 3.2 Å, is longer than that explored in fully hydrated powder (15, 16) and in the integral membrane protein bacteriorhodopsin (17, 21), which present sphere radii between 0.8 Å and 1.7 Å. In contrast, the volume explored by the atoms in cell macromolecules is similar or smaller than the volume explored by the atoms from proteins in solution, depending on the solution concentration. The sphere radii have been found to be: 2.5 Å for a concentrated solution of 244 mg/ml of dihydrofolate reductase (DHFR) at 285 K (35); 4.1 Å and 4.4 Å for solutions of 60 mg/ml of myoglobin and lysozyme, respectively, at 293 K (16); 3.6 Å for a solution of 85 mg/ml of bovine pancreatic trypsin inhibitor (BPTI) at ambient temperature (34). If we exclude the DHFR case, the extrapolated HWHM at $Q^2 = 0$ is smaller for cell macromolecules compared to the value of about 150 μeV found for proteins in solution and in membrane (16, 21), and higher than the value of about 70 μeV extracted for proteins in fully hydrated powder (15, 16). We recall that lower HWHM correspond to longer correlation times and reflects slower motions. Considering both the length- and time-scales, the average diffusive motions explored in a few ps inside cell macromolecules lie between those found for proteins in hydrated powder and in solution.

Slow internal motions

By using the 17 μeV energy resolution of the IRIS spectrometer, slower processes belonging to a time-scale of a few tens of ps were isolated. As for IN6, the global motions do not contribute to the scattering signal on IRIS. The IRIS spectra were fitted with two Lorentzian functions using Eq. 4, 5. The HWHM of the broad Lorentzian, Γ_{fast}, is plotted in Fig. 4, for the 280 K and 300 K temperatures. It revealed a similar profile to that found for IN6 data fitted with one Lorentzian: at low Q^2, Γ_{f0} is about 100 μeV at the two temperatures; Γ_{fast} increases at larger Q^2 values up to $\Gamma_{f\infty}$ values of 140 μeV and 180 μeV, at 280 K and 300 K respectively, which correspond to correlation times of about 4.7 ps and 3.7 ps, respectively.

The broad Lorentzian, therefore, was attributed to the fast internal motions isolated previously on IN6 with the single Lorentzian approach.

The HWHM of the sharp Lorentzian, Γ_{slow}, plotted in Fig. 5, showed a Q^2-independent profile, indicating reorientational motions. Γ_{slow} had a mean value of about 14 μeV at the two temperatures, corresponding to a correlation time of 44 ps. The sharp Lorentzian arises from slower internal motions, compared to the fast processes characterized on IN6. The slow processes can be for example stochastic reorientations of large molecular subunits, such as polypeptide side chains, fatty acid chains or other molecular subunits, as well as rotational motions of smaller groups, such as protons in methyl groups. Molecular dynamics simulations on hydrated lysozyme at 295 K have shown that methyl groups presented a wide range of associated correlation times, with a mean value of about 75 ps (14). The *Q*-dependence of the QISF associated to the slow motions (*figure not shown*) revealed a profile that suggests a two-site jump diffusion model. It is in good agreement with a previous work on purple membrane (18), in which Fitter and coworkers have investigated internal molecular motions of bacteriorhodopsin at 297 K, using the same energy resolution on IRIS (18). They have isolated a "slow" proton population, whose motions were described by a two-site jump diffusion model, with associated relaxation times, $2/\Gamma_{f\infty}$, of 80-100 ps. It corresponds to correlation times of about 40-50 ps, which are similar to the correlation times found for *E. coli*.

Very slow internal motions and macromolecular self-diffusion

Very slow internal motions were separated from macromolecular self-diffusion using the energy resolution of the IN16 spectrometer (FWHM = 0.9 μeV), which gives access to characteristic times up to 1 ns. The apparent self-diffusion coefficient, *D*, of hemoglobin in red blood cells have been found to be about $1.2 \cdot 10^{-7}$ cm^2/s in D_2O at 310 K (25). Hemoglobin is the main component of red blood cells, with a molecular mass of 64 kDa and a concentration *ca.* 330 mg/ml close to that in the cell cytoplasm (26). Cellular macromolecules present a distribution of molecular masses, going from a few tens to a few thousands of kDa. Considering similar macromolecular concentrations, the apparent self-diffusion coefficient of *E. coli* macromolecules, mainly proteins, is expected to be of the same order than the value found for hemoglobin in red blood cells. The QENS broadening arising from global motions of cellular macromolecules coincides therefore with the IN16 energy resolution, and has to be taken into account to extract very slow internal motions from the scattering signal. The global and internal motions were each well described by a single Lorentzian and Eq. 2 described in *materials and methods* simplified as follows:

$$S_{calc}(\mathbf{Q},\omega) = DW\left[A_{self}(\mathbf{Q})\,L(\Gamma_{self},\omega) + A_{broad}(\mathbf{Q})\,L(\Gamma_{very\text{-}slow} + \Gamma_{self},\omega)\right] \quad (8)$$

The broad Lorentzian arises mainly from the internal contribution, $\Gamma_{very\ slow}$, and is broadened by the self-diffusion contribution, Γ_{self}, as described in Eq. 8. The results of the fit obtained using Eq. 8 are shown in Fig. 6.

The HWHM of the sharp Lorentzian, Γ_{self}, is plotted in Fig. 7. The Γ_{self} profile revealed long-range translational motions, as indicated by the increase of the linewidth with *Q* and the extrapolation to 0 for $Q \rightarrow 0$. Γ_{self} increased up to about 0.5 μeV at 284 K and 0.75 μeV at 303 K. The linewidth was well fitted using a jump diffusion model, which describes diffusion between sites with a mean residence time, τ_0, at each site (29). Γ_{self} follows (29):

$$\Gamma_{self} = \frac{DQ^2}{1 + DQ^2\tau_0} \quad (9)$$

where D represents the apparent translational diffusion coefficient. We found D = (0.85 ± 0.15) x 10^{-7} cm^2/s, τ_0 = 0.97 ± 0.08 ns at 284 K, and D = (1.06 ± 0.11) x 10^{-7} cm^2/s, τ_0 = 0.59 ± 0.04 ns at 303 K. The values are consistent with the value of 1.2 · 10^{-7} cm^2/s found for hemoglobin in red blood cells at 310 K (25). The average characteristic distance between two jumps was found to be 2.2 Å at 284 K and 1.9 Å at 303 K, which are reasonable values for macromolecules with an average radius of gyration of a few tens of Å. These values are also in good agreement with the value of 1.0 Å found by Busch and coworkers at 293 K, for myoglobin in crowded solutions with a concentration close to the cell cytoplasm (32). We attributed, therefore, the sharp Lorentzian to the apparent self-diffusion of macromolecules in the *E. coli* interior.

The HWHM of the broad Lorentzian, corrected for the broadening arising from the self-diffusion contribution, was extracted and is plotted in Fig. 8; $\Gamma_{very\ slow}$ revealed a Q^2-independent profile. The mean HWHM is 7.0 μeV at 284 K and 7.3 μeV at 303 K, which correspond to correlation times of about 94 ps and 90 ps, respectively. $\Gamma_{very\ slow}$ arises from very slow internal motions from all protons participating for example in librations of buried groups, relative displacements of globular domains, sugar conformational changes, or RNA global bending (36). The correlations times found for *E. coli* macromolecules are close to those found in previous studies on proteins in concentrated solutions (32) or in membrane stacks (20) at similar energy resolutions: by using the HFBS spectrometer (FWHM = 0.8 μeV) at NIST (37), Busch and coworkers have found a HWHM = 10 μeV, which corresponds to a correlation time of 65 ps, for myoglobin in concentrated solution with a volume fraction of 0.4 (32); by using the IN10 spectrometer (FWHM = 1.8 μeV) at the ILL, Fitter and coworkers have evaluated a mean HWHM = 5.5 μeV for bacteriorhodopsin in purple membrane stacks, which corresponds to a correlation time of 120 ps (20).

Influence of the cellular environment on macromolecular dynamics

The QENS study on *E. coli* led to the first dynamical mapping of macromolecular dynamics *in vivo,* on the full ps-to-ns time-scale accessible through neutron scattering. The large panel of internal macromolecular motions as well as the self-diffusion of cell macromolecules were explored and characterized *in vivo*.

The analysis of the internal motions permitted the separation between a fast ps process and slower (tens of ps) processes. Physiological internal motions were found to be a combination of reorientational and restricted jump diffusion motions. The comparison with previous *in vitro* studies revealed interesting differences between physiological internal motions and those found in hydrated powders or in solution. Both internal molecular flexibility and diffusion rates occurring in a few ps are increased significantly in the cell interior compared to fully hydrated powders. The result showed that the large amount of cell water plays a decisive role in physiological internal dynamics. The effect of water, which was observed mainly on the ps time-scale associated to hydrogen bond breaking and formation, suggested that the cell water hydrogen bond network influences the hydrogen bond dynamics in macromolecular structures, and contributes to physiological structural flexibility. However, the smaller values found for the parameters measured *in vivo* compared to those measured in solution suggested that weak forces due to the vicinity of macromolecules attenuate the lubricating effect of water.

The work on *E. coli* demonstrated that powders and solutions do not accurately picture the physiological dynamical behaviour of macromolecules. It underlined the central role of cellular water as well as the slight influence of macromolecular crowding on internal macromolecular dynamics in living cells. The study suggested that the intracellular

complexity participates in physiological functional dynamics necessary to biological activity.

ACKNOWLEDGMENTS

We thank the ILL and the ISIS neutron facilities for providing beamtime. We acknowledge Dr. M. Koza and Dr. B. Frick (ILL, France) for assistance with the IN6 and IN16 measurements, and Dr. S. Rols (ILL, France) for help with the QENS_fit routine handling. We thank Dr. M.F. Telling (ISIS, Rutherford Laboratory, U.K.) for help with the IRIS measurements and the MODES program. M.J. acknowledges support of a French Science Ministry doctoral fellowship. M.T. acknowledges the ILL, the CNRS and the IBS (UMR 5075) for financial support of this work. The research was supported by the European Union, under the two contracts for the Deuteration Laboratory (ILL, France), HPRI-CT-2001-50035 and RII3-CT-2003-505925, and by the Integrated Infrastructure Initiative for Neutron Scattering and Muon Spectroscopy (NMI3).

REFERENCES

1. Brooks, C. L., M. Karplus, and B. M. Pettitt. 1988. Proteins: a theoretical perspective of dynamics, structure, and thermodynamics. Advan. Chem. Phys. 71:1-249.
2. Austin, R. H., K. W. Beeson, L. Eisenstein, H. Frauenfelder, and I. C. Gunsalus. 1975. Dynamics of ligand binding to myoglobin. Biochemistry 14:5355-5373.
3. Rousseau, F., and J. Schymkowitz. 2005. A systems biology perspective on protein structural dynamics and signal tranduction. Curr. Opin. Struct. Biol. 15:23-30.
4. Tousignant, A., and J. N. Pelletier. 2004. Protein motions promote catalysis. Chem. Biol. 11:1037-1042.
5. Jimenez, R., G. Salazar, J. Yin, T. Joo, and F. E. Romesberg. 2004. Protein dynamics and the immunological evolution of molecular recognition. Proc. Natl. Acad. Sci. U. S. A. 101:3803-3808.
6. Gabel, F., D. Bicout, U. Lehnert, M. Tehei, M. Weik, and G. Zaccai. 2002. Protein dynamics studied by neutron scattering. Q. Rev. Biophys. 35:327-367.
7. Frauenfelder, H., F. Parak, and R. D. Young. 1988. Conformational substates in proteins. Annual Review of Biophysics and Biophysical Chemistry 17:451-479.
8. Smith, J. C. 1991. Protein dynamics: comparison of simulations with inelastic neutron scattering experiments. Q. Rev. Biophys. 24:227-291.
9. Andreani, C., A. Filabozzi, F. Menzinger, A. Desideri, A. Deriu, and D. Di Cola. 1995. Dynamics of hydrogen atoms in superoxide dismutase by quasielastic neutron scattering. Biophys. J. 68:2519-2523.
10. Dellerue, S., A. J. Petrescu, J. C. Smith, and M. C. Bellissent-Funel. 2001. Radially softening diffusive motions in a globular protein. Biophys. J. 81:1666-1676.
11. Doster, W., S. Cusack, and W. Petry. 1989. Dynamical transition of myoglobin revealed by inelastic neutron scattering. Nature 337:754-756.
12. Fitter, J. 1999. The temperature dependence of internal molecular motions in hydrated and dry α-amylase: The role of hydration water in the dynamical transition of proteins. Biophys. J. 76:1034-1042.
13. Paciaroni, A., A. Orecchini, S. Cinelli, G. Onori, R. E. Lechner, and J. Pieper. 2003. Protein dynamics on the picosecond timescale as affected by the environment: a quasielastic neutron scattering study. Chemical Physics 292:397-404.
14. Roh, J. H., J. E. Curtis, S. Azzam, V. N. Novikov, I. Peral, Z. Chowdhuri, R. B. Gregory, and A. P. Sokolov. 2006. Influence of hydration on the dynamics of lysozyme. Biophys. J. 91:2573-2588.

15. Zanotti, J. M., M. C. Bellissent-Funel, and J. Parello. 1997. Dynamics of a globular protein as studied by neutron scattering and solid-state NMR. Physica B 234:228-230.
16. Pérez, J., J. M. Zanotti, and D. Durand. 1999. Evolution of the internal dynamics of two globular proteins from dry powder to solution. Biophys. J. 77:454-469.
17. Fitter, J., O. P. Ernst, T. Hauß, R. E. Lechner, K. P. Hofmann, and N. A. Dencher. 1998. Molecular motions and hydration of purple membranes and disk membranes studied by neutron scattering. Eur. Biophys. J. 27:638-645.
18. Fitter, J., R. E. Lechner, G. Büldt, and N. A. Dencher. 1996. Internal molecular motions of bacteriorhodopsin: hydration-induced flexibility studied by quasielastic incoherent neutron scattering using oriented purple membranes. Proc. Natl. Acad. Sci. U. S. A. 93:7600-7605.
19. Fitter, J., R. E. Lechner, G. Büldt, and N. A. Dencher. 1996. Temperature dependence of molecular motions in the membrane protein bacteriorhodopsin from QINS. Physica B 226:61-65.
20. Fitter, J., R. E. Lechner, and N. A. Dencher. 1997. Picosecond molecular motions in bacteriorhodopsin from neutron scattering. Biophys. J. 73:2126-2137.
21. Fitter, J., R. E. Lechner, and N. A. Dencher. 1999. Interactions of hydration water and biological membranes studied by neutron scattering. Journal of Physical Chemistry B 103:8036 -8050.
22. Ellis, R. J. 2001. Macromolecular crowding: an important but neglected aspect of the intracellular environment. Current Opinion in Structural Biology 11:114-119.
23. Elowitz, M. B., M. G. Surette, P. E. Wolf, J. B. Stock, and S. Leibler. 1999. Protein mobility in the cytoplasm of *Escherichia coli*. Journal of Bacteriology 181:197-203.
24. Luby-Phelps, K. 2000. Cytoarchitecture and physical properties of cytoplasm: volume, viscosity, diffusion, intracellular surface area. International Review of Cytology 192:189-221.
25. Doster, W., and S. Longeville. 2007. Microscopic diffusion and hydrodynamic interactions of hemoglobin in red blood cells. Biophys. J. 93:1360-1368.
26. Ellis, R. J. 2001. Macromolecular crowding: obvious but underappreciated. Trends in Biochemical Sciences 26:597-604.
27. MODES, a graphic user interface for IRIS data analysis http://www.isis.rl.ac.uk/molecularspectroscopy/iris/.
28. LAMP, the Large Array Manipulation Program. http://wwwold.ill.fr/data_treat/lamp/front.html.
29. Bée, M. 1988. Quasielastic Neutron Scattering: Principles and Applications in Solid State Chemistry, Biology and Materials Science. Adam Hilger, Philadelphia.
30. Tehei, M., B. Franzetti, D. Madern, M. Ginzburg, B. Z. Ginzburg, M. T. Giudici-Orticoni, M. Bruschi, and G. Zaccai. 2004. Adaptation to extreme environments: macromolecular dynamics in bacteria compared *in vivo* by neutron scattering. EMBO Rep. 5:66-70.
31. Madigan, M. T., J. M. Martinko, and J. Parker. 2000. Brock Biology of Microorganisms. Prentice Hall.
32. Busch, S., W. Doster, S. Longeville, and V. G. Sakai. 2007. Microscopic protein diffusion at high concentration. MRS Bulletin. Quasielastic Neutron Scattering Conference 2006, p.117-116.
33. Volino, F., and A. J. Dianoux. 1980. Neutron incoherent scattering law for diffusion in a potential of spherical symmetry: general formalism and application to diffusion inside a sphere. Molecular Physics 41:271-279.

34. Appavou, M. S., G. Gibrat, and M. C. Bellissent-Funel. 2006. Influence of pressure on structure and dynamics of bovine pancreatic trypsin inhibitor (BPTI): small angle and quasi-elastic neutron scattering studies. Biochim. Biophys. Acta 1764:414-423.
35. Tehei, M., J. C. Smith, C. Monk, J. Ollivier, M. Oettl, V. Kurkal, J. L. Finney, and R. M. Daniel. 2006. Dynamics of immobilized and native *Escherichia coli* dihydrofolate reductase by quasielastic neutron scattering. Biophys. J. 90:1090-1097.
36. Mc Cammon, J. A., and S. C. Harvey. 1987. Dynamics of proteins and nucleic acids. Cambridge University Press, New York.
37. Meyer, A., R. M. Dimeo, P. M. Gehring, and D. A. Neumann. 2003. The high-flux backscattering spectrometer at the NIST Center for Neutron Research. Review of Scientific Instruments 74:2759-2777.

TABLES

Table 1: Chemical composition of *E. coli* (from (31)).

Molecules	**Percent of dry weight**
Total macromolecules	**96**
Protein	55
Polysaccharide	5
Lipid	9.1
Lipopolysaccharide	3.4
DNA	3.1
RNA	20.5
Total monomers	**3**
Amino acids and precursors	0.5
Sugars and precursors	2
Nucleotides and precursors	0.5
Inorganic ions	**1**
Total	**100**

FIGURE LEGENDS

Figure 1: IN6 QENS data of native *E. coli* containing D_2O. QENS spectra at Q = 1.5 Å^{-1}, at T = 280 K (*left*) and T = 300 K (*right*). The fit for each spectrum was performed in the quasi-elastic region for -1.5 meV < $\hbar\omega$ < 1.5 meV. The data are indicated by the triangles; the total fitted curve (*bold line*) was obtained using Eq. 4, 5 with a single Lorentzian function. The elastic peak is represented by a dotted line. The Lorentzian is represented by a dash-dotted line. The highest intensity values (*top of the frame*) in both figures correspond to about one third of the total intensity at $\hbar\omega$=0.

Figure 2: IN6 data. HWHM of the single Lorentzian, Γ_{fast}, as a function of Q^2, at 280 K (*squares*) and 300 K (*triangles*).

Figure 3: IN6 data. Elastic incoherent structure factor (EISF) as a function of Q, at 280 K (*squares*) and 300 K (*triangles*).

Figure 4: IRIS data. HWHM of the broad Lorentzian, Γ_{fast}, as a function of Q^2 at 280 K (*squares*) and 300 K (*triangles*).

Figure 5: IRIS data. HWHM of the sharp Lorentzian, Γ_{slow}, as a function of Q^2, at 280 K (*squares*) and 300 K (*triangles*).

Figure 6: IN16 QENS data and applied fits for native *E. coli* containing D_2O. QENS spectra at Q = 1.3 Å^{-1}, at T = 284 K (*left*) and T = 303 K (*right*). The fit for each spectrum was performed in the quasielastic region for -12 μeV < $\hbar\omega$ < 12 μeV. The data are indicated with the associated error bars. The bold line is the total fitted curve obtained using Eq. 4, 8. The broad Lorentzian is shown by a dot-dash line and the sharp Lorentzian by a dash line.

Figure 7: IN16 data. HWHM of the sharp Lorentzian, Γ_{self}, as a function of Q^2 at 284 K (*squares*) and 303 K (*triangles*).

Figure 8: IN16 data. HWHM of the broad Lorentzian corrected for the self-diffusion contribution as a function of Q^2, at 284 K (*squares*) and 303 K (*triangles*).

Fig. 1 (*left*)

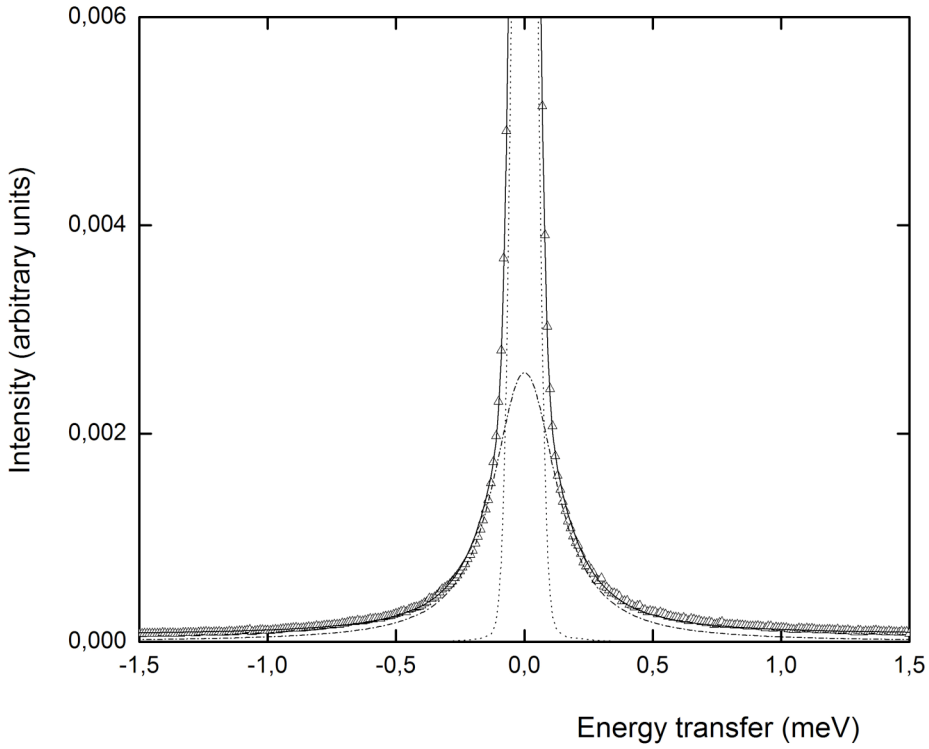

Fig. 1 (*right*)

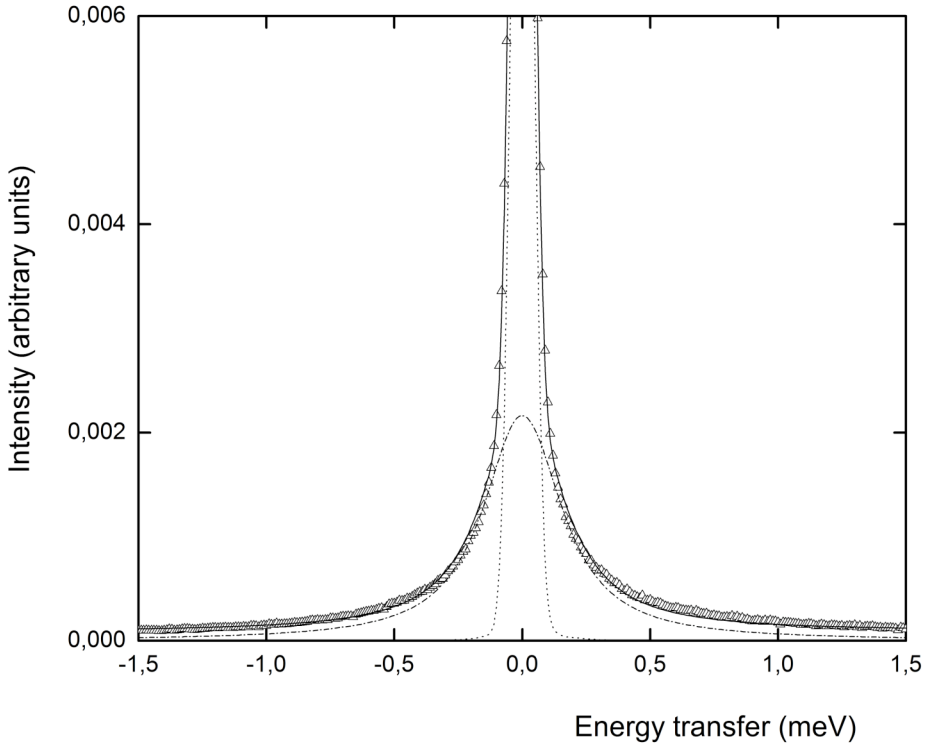

Fig. 2

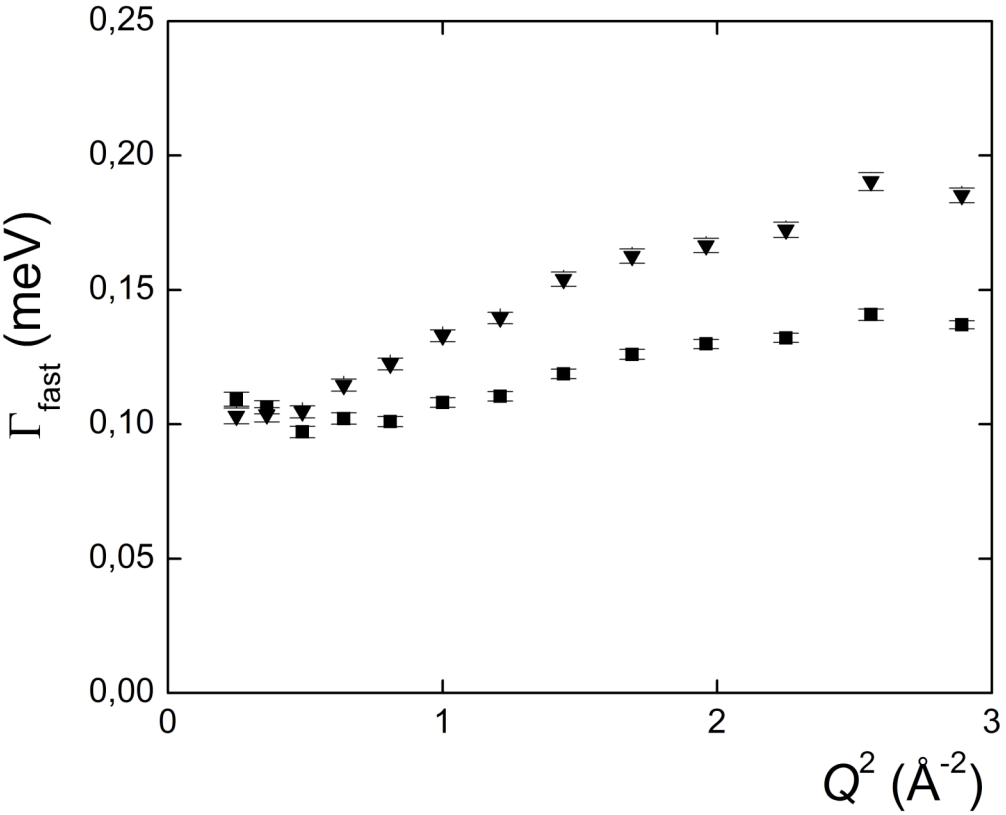

Fig. 3

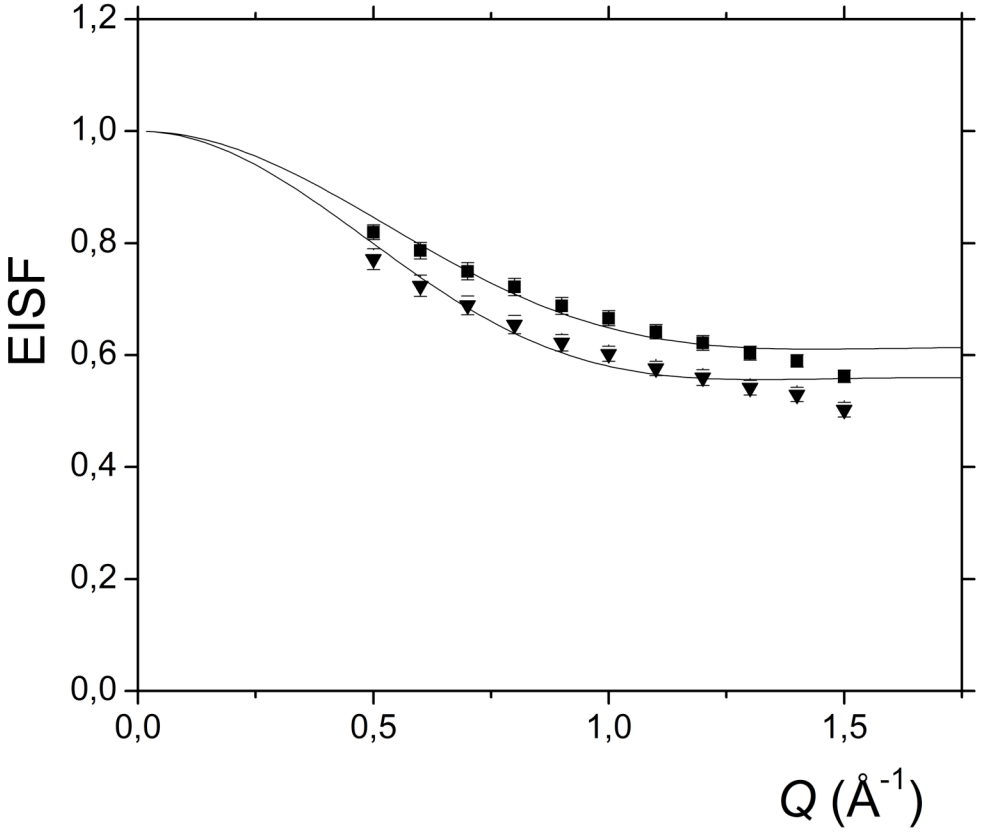

Fig. 4

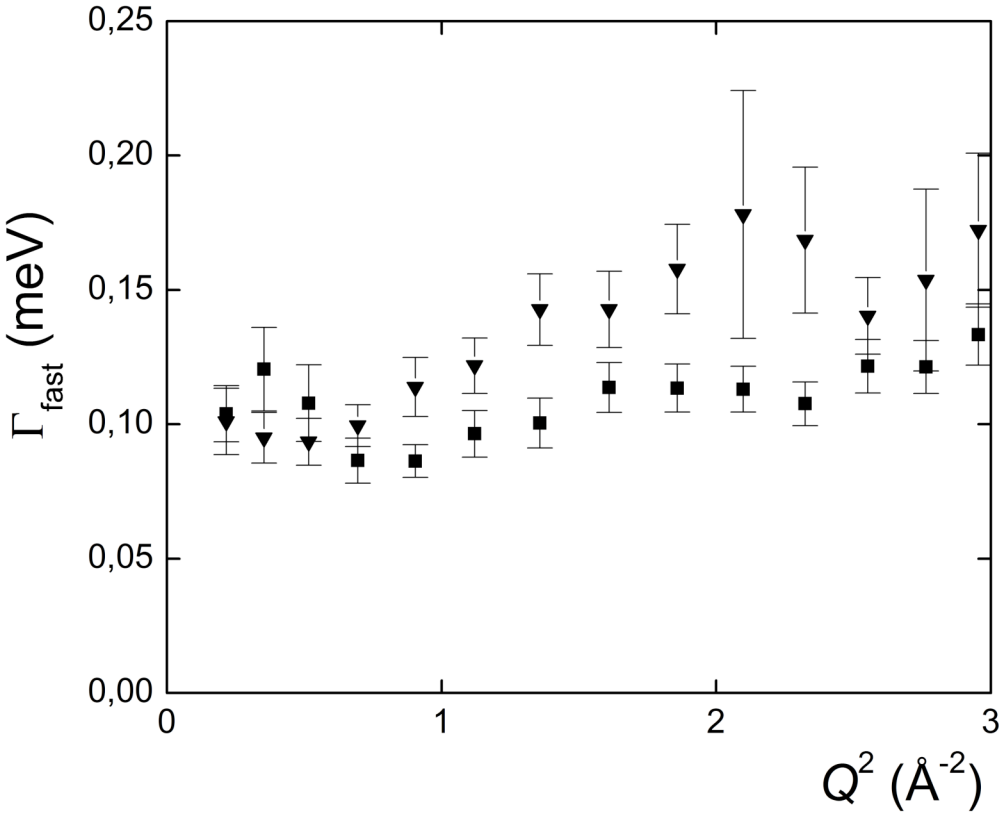

Fig. 5

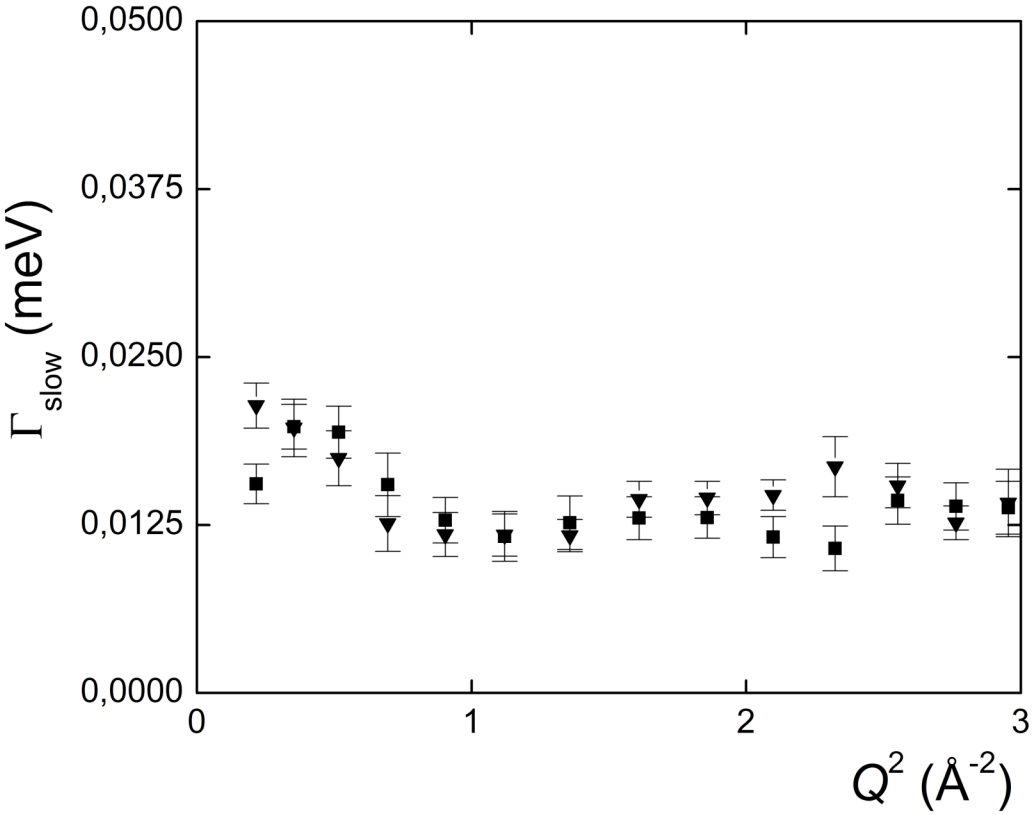

Fig. 6 (*left*)

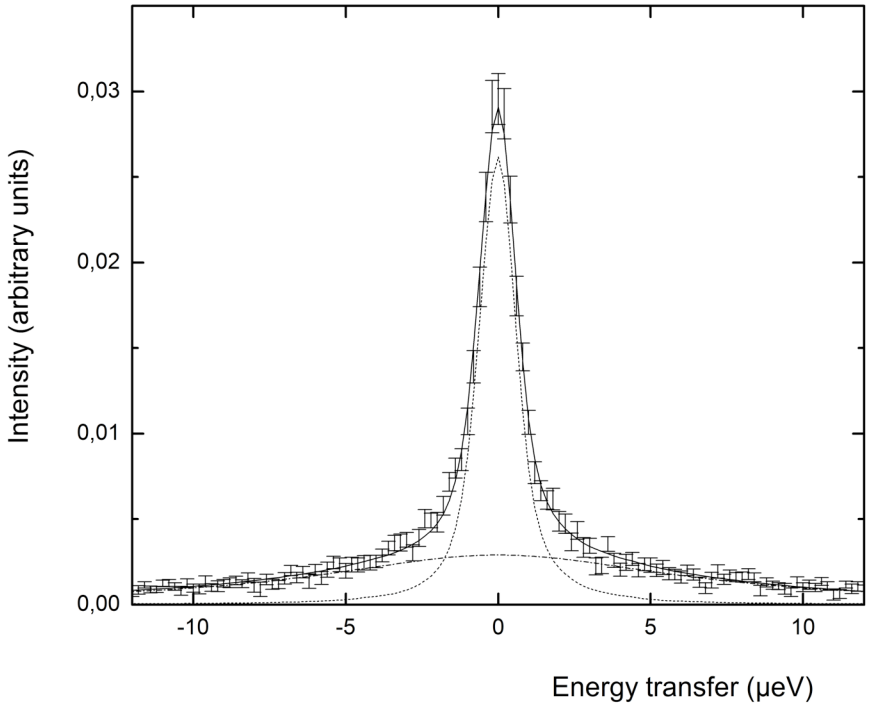

Fig. 6 (*right*)

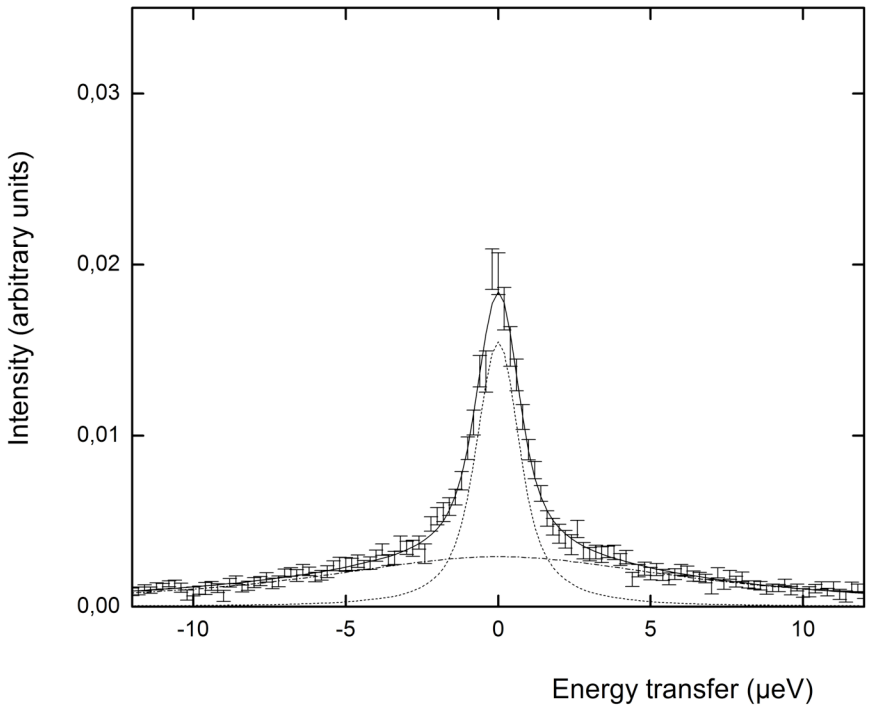

Fig. 7

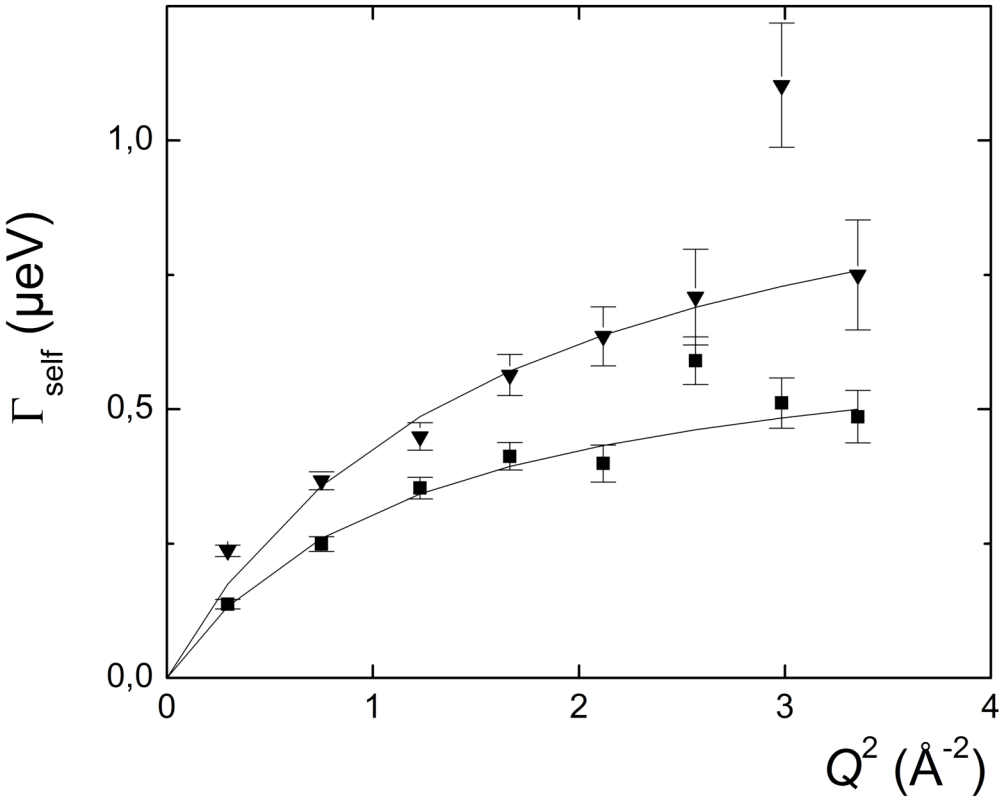

Fig. 8